Performance analysis of wind turbines with leading-edge erosion and erosion-safe mode operation

Barfknecht, N.; Kreuseler, M.; De Tavernier, D.; Von Terzi, D.

DOI
10.1088/1742-6596/2265/3/032009

Publication date
2022

Document Version
Final published version

Published in
Journal of Physics: Conference Series

Performance analysis of wind turbines with leading-edge erosion and erosion-safe mode operation

Performance analysis of wind turbines with leading-edge erosion and erosion-safe mode operation

N Barfknecht, M Kreuseler, D de Tavernier, D von Terzi
Delft University of Technology, Wind Energy, Kluyverweg 1, Delft, The Netherlands
E-mail: n.barfknecht@tudelft.nl

Abstract. For offshore wind turbines, Leading-Edge Erosion (LEE) due to rain is posing a serious risk to structural integrity and can lead to a performance loss of the order of a few percent of the Annual Energy Production (AEP). A proposed mitigation strategy is the so-called Erosion-Safe Mode (ESM). In this work, the AEP losses caused by LEE or by operating in the ESM are compared for two reference turbines, i.e. the IEA 15MW and the NREL 5MW turbines. For both turbines, the performance is evaluated in uniform and sheared inflow conditions. The effects of erosion are modeled by creating clean and rough airfoil polars in XFOIL. It is assumed that erosion occurs once a critical blade element section speed is exceeded. Power curves for LEE and ESM are calculated by using the free-wake vortex method CACTUS. Results show that LEE negatively affects the power production below rated capacity, while operating in ESM predominantly sheds performance at rated power of the turbine. This study, therefore, shows that a break-even point for the ESM exists. The AEP loss due to erosion can be successfully mitigated with the ESM at sites with low mean wind speed, however, at sites with higher mean wind speed, operation with erosion leads to a lower AEP loss. The break-even point shows little sensitivity to the blade design and to mean shear variations, but strongly depends on the frequency ESM needs to be applied. The latter is driven by the predicted amount of damaging rain events. In conclusion, erosion-optimal operation is strongly governed by the site characteristics and much less by turbine design, and the viability of an ESM strategy can be significantly expanded by a better understanding of blade damage mechanisms and improved forecasting of the related weather events.

1. Introduction

For offshore wind turbines, Leading-Edge Erosion (LEE) due to rain is posing a serious risk to structural integrity. Moreover, LEE has been observed to produce a significant performance loss of the order of a few percent of the Annual Energy Production (AEP) [1]. The cause for this loss is an earlier transition from a laminar to a turbulent boundary layer over the airfoil initiated by increased surface roughness. Typical mitigation techniques include coatings, tapes, or shields to protect the blade from erosion. Most of these techniques also incur a performance loss in the variable speed region of the power curve of the order of, but commonly lower than, an eroded blade. An alternative method proposed in the literature is to operate in an Erosion-Safe Mode (ESM). Here, the tip speed of the turbine is limited during certain weather conditions to avoid erosion [2]. However, the ESM may also lead to performance reductions, but more likely at rated power. Moreover, field measurements have shown that the performance loss caused by LEE varies with the stability state of the atmospheric boundary layer [3], i.e. for different levels of shear and turbulence intensity. In general, the trade-off between design and operation of

turbines to minimize performance losses due to erosion or its mitigation is not well understood. This is, in particular, true for the next generation of giant turbines.

This work aims to compute and compare the AEP loss caused by leading-edge erosion or by operating in the ESM. Two offshore reference turbines, the IEA 15MW and the NREL 5MW turbine, will be analysed using lower-fidelity methods [4, 5]. The performance is evaluated in uniform and sheared inflow conditions for both turbines. The main focus is to identify the major trends and trade-offs between operating with LEE or operating in an ESM. The precise quantification of the performance loss is not the aim of this study.

2. Methodology

The main tool pipeline used throughout this paper is built using XFoil [6] and CACTUS [7]. The flowchart of the entire procedure is given in Figure 1 and explained block-wise below.

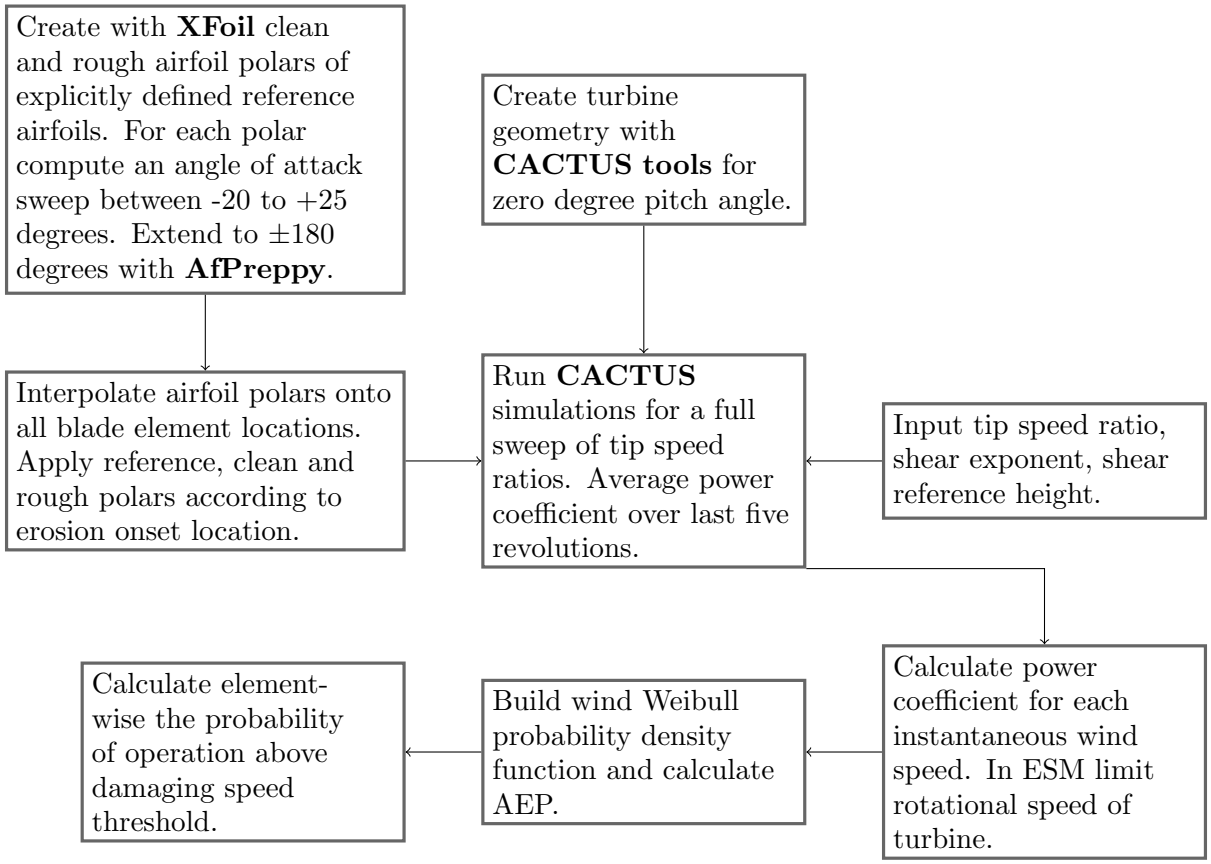

Figure 1: Flowchart of methodology used throughout this paper to compute data.

XFoil: For clean conditions, polars are provided with the definition of the reference turbines. This is not the case for rough, eroded blades. As such we have re-defined both the clean and rough polars, for consistency. For this purpose, XFoil is used.

Eroded damage is modeled in XFoil by inducing boundary layer transition at fixed locations close to the leading-edge (1% top and 10% bottom for positive angle of attack (AoA), flipped for negative AoA). Note that this approach only considers the airfoil's performance reduction due to the early transition but not due to the thickening of the boundary-layer from the airfoil roughness itself. Therefore this study only considers erosion damage typical for moderately

eroded blades. Modeling heavily eroded blades with deep surface imperfections requires high-order modeling techniques that are out of the scope of this work. For the simulations a fixed Reynolds number of 8.5 million was chosen for the NREL 5MW turbine and 11.5 million for the IEA 15MW turbine. The Reynolds numbers were determined by weighing the local Reynolds number of every blade element by its contribution to the total power coefficient. The Reynolds number was kept constant for both turbines throughout the entire study. Thus independency of the polars with respect to the Reynolds number for different wind speeds, rotational speeds of the turbine, and blade location was assumed. The same assumption has been made for the Mach number, which was set to zero. Since the integral boundary-layer method is questionable at high Reynolds numbers, a set of polars is generated with varying N-factors in the e^N-method. The N-factor represents the airfoil's sensitivity to promote turbulent transition and thus, to some extent, may capture the uncertainty in predicting the free transition location at high Reynolds numbers. The standard value chosen for this study in clean blade conditions is $N = 9$, while other values equal to 7, 8 and 10 are considered as well.

The airfoils are discretized with about 150 to 250 panels in XFoil. For each computed polar, the number of panels has been tuned carefully by trial and error to ensure complete convergence over the range from -20 to +25 degrees angle of attack. The polars were extended to the full ±180 range by using AirfoilPreppy's Viterna's method [8, 9].

CACTUS: The blade reference discretization according to the reference turbines' ontology files was preserved (60 points for IEA 15MW, 48 points for NREL 5MW). Two strategies have been used to apply the individual airfoil polars to their respective location along the blade. Consistent with the NREL 5MW's turbine definition, the airfoils, and thus also the polars, have been kept constant along the stations. Consistent with the IEA 15MW's definition, the polars were linearly interpolated between the stations. For the cylindrical inboard sections of both turbines' blades, the reference polars have been used. Additionally, for the most inboard airfoil of the IEA 15MW turbine, the SNL-FFA-W3-500, the reference polar has been used as well due to its high thickness. For every eroded simulation, a specific erosion onset location along the blade was assumed. The CACTUS input airfoils along every station were assembled by using the clean polars inboard the erosion location and the eroded polars outboard of the erosion location.

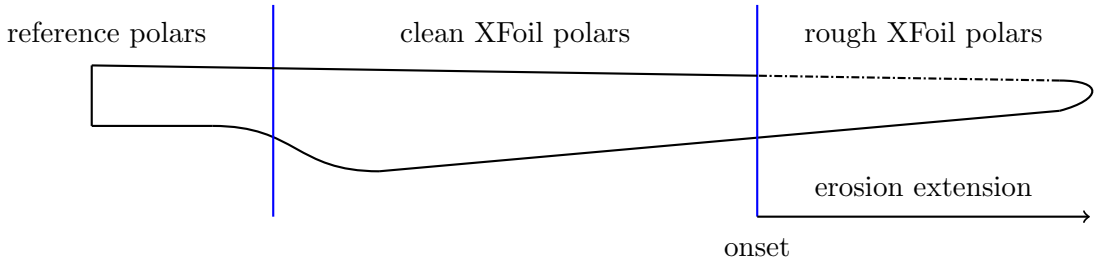

Figure 2: Use of reference and XFoil airfoil polars along the blade in the CACTUS simulations.

The CACTUS turbine geometries were created by using the horizontal-axis wind turbine (HAWT) tool from CACTUS-tools [10]. A convergence study on the time steps and number of rotations was performed to ensure good numerical quality of the CACTUS simulations. Absolute errors in the power coefficient are in the range of <1E-4 for TSR < 10 and <1E-3 for TSR > 10. A discretization of 40 times step per revolution is used, vortex elements are cut off after they have reached five rotor radii. The simulations were run for 50 rotations at design TSR and up to 90 rotations at maximum TSR. Sheared inflow is modeled by using CACTUS' built in inflow power law together with different shear exponents. The shear reference height was set to the hub height.

Simulation with turbine controller: The power coefficients obtained from the CACTUS simulations were averaged over the last five revolution. For the blade element data, the data were averaged over all blades over the last simulated revolutions. Subsequently, the power coefficients were fed to the steady state turbine controller. The IEA 15MW controller was modified so that it only operates at zero pitch angle in order to limit the amount of CACTUS simulations that were needed to be carried out. In ESM operation, the controller was adjusted according to two rules: 'rotational' (ROT) and 'relative' (REL). In the rotational mode the assumption was made that the rain impact velocity is equal to the rotational velocity component of the blade, whereas for the relative mode also the freestream hub-height inflow component was taken into account according to $U_{\mathrm{ESM,REL}} = \mathrm{norm}(U_{\mathrm{in}}, U_{\mathrm{rot}})$. Here induction is ignored. ROT and REL represent the limiting cases of droplet behavior. ROT corresponds to a droplet that does not get advected with the wind velocity, while REL corresponds to a droplet that gets perfectly advected with the wind velocity. To limit the amount of free variables and complexity, the droplet terminal velocity has been neglected. In the case of ESM operation, the tip speed of the turbine is limited so that the droplet impact speed, according to the ROT or REL mode, stays below a defined damage threshold.

Calculation of AEP (loss): The calculation of AEP is carried out for sites with different mean wind speeds at hub height assuming a representative Weibull wind distribution with a shape parameter of two. A combined power curve is composed by weighting the clean and ESM power curves according to the assumed damaging rain frequency. The AEP loss was calculated as the relative error between rough and clean cases, with the clean case being the baseline. A possible correlation between site mean wind speed and rain frequency was not considered. While important for exact quantification of AEP losses it is deemed not to have a significant impact on the trade-offs between operation with LEE and operating in an ESM.

3. Results

Figure 3 shows the lift coefficient as a function of the angle of attack for the most outboard airfoils of the IEA 15MW and NREL 5MW turbine in clean and rough conditions. The differences between the clean and rough lift polars are relatively small. This could be expected since the airfoils are operating at high Reynolds numbers, meaning the flow over the airfoil suction side is mostly turbulent even at small angles of attack. Forcing the flow to be turbulent close to the leading edge will only marginally affect the airfoil's performance. This easily follows from Figure 4, which indicates the location of the transition point from laminar to turbulent flow on the suction side of the airfoils, both for the clean and rough cases.

At low angles of attack, the largest differences may be identified between the clean and rough case. Here, free transition on the upper surface occurs downstream of the forced transition location set at 1% of chord (as explained in Section 2). With increasing angle of attack, the location of free transition moves upstream. The NREL curve is concave, meaning that the transition point moves gradually forward with increasing angles of attack. In contrast, the IEA curve is convex. The transition point stays fairly constant until it abruptly shifts all the way to the leading edge. The IEA turbine shows convergence of the free and forced transition locations at an angle of attack of about four degrees, while the NREL gradually converges between zero and four degrees. At higher angles of attack, where the free and forced transition locations overlap, a small difference between both curves can still be identified in Figure 3. This may no longer be attributed to the forced transition on the suction side, but it can be related back to the forced transition on the pressure side. However, this contribution is significantly smaller. Although not shown is this paper, similar observations can be made on the drag polar. Here, the effect on drag and thus also the lift-to-drag ratio is more pronounced. Nevertheless, small deviations in lift and drag may have significant effects on the turbine performance.

Figure 4 also presents the sensitivity of the transition location as a function of the N-factor.

Note that high N-factors result in a free-transition location farther downstream. This implies that the effects of early transition on the airfoil's performance will be more pronounced at higher N-factors.

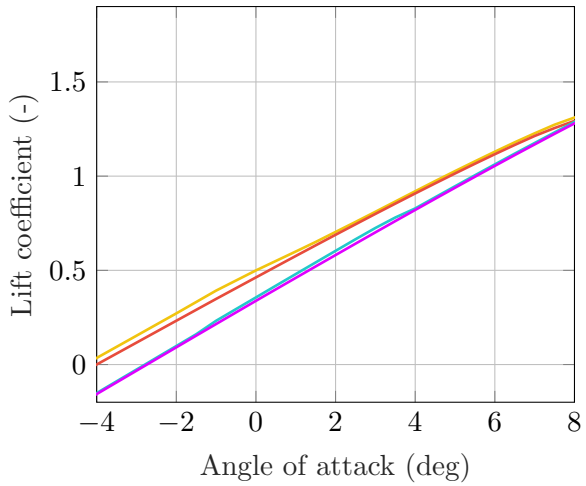

Figure 3: $C_l - \alpha$ for most outboard airfoils. FFA-W3-211 for IEA. NACA 64-618 for NREL. N=9. IEA: clean: —, rough: — NREL: clean: —, rough: —

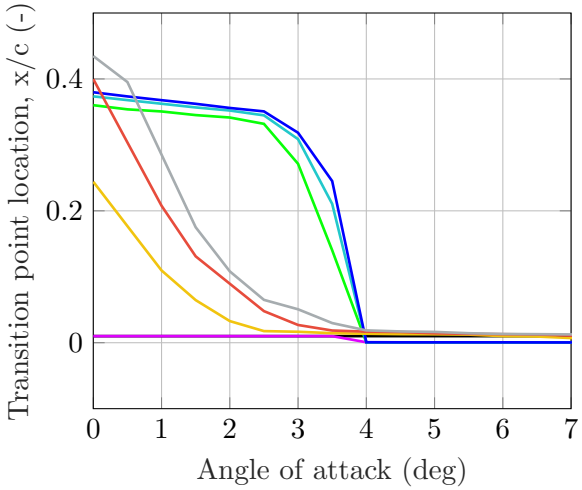

Figure 4: Transition point location on suction side for most outboard airfoils. FFA-W3-211 for IEA. NACA 64-618 for NREL. IEA: N7: —, N9: —, N10: —, rough: — NREL: N7: —, N9: —, N10: —, rough: —

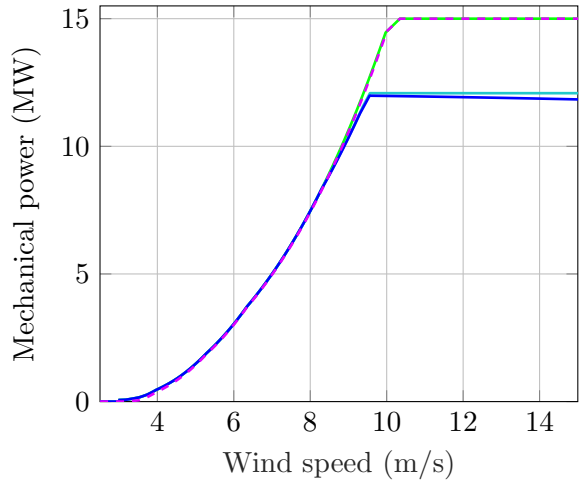

Figure 5: Power curve of IEA 15MW turbine. Clean: —, rough: - - -, ESM ROT 75 m/s: —, ESM REL 75 m/s: —

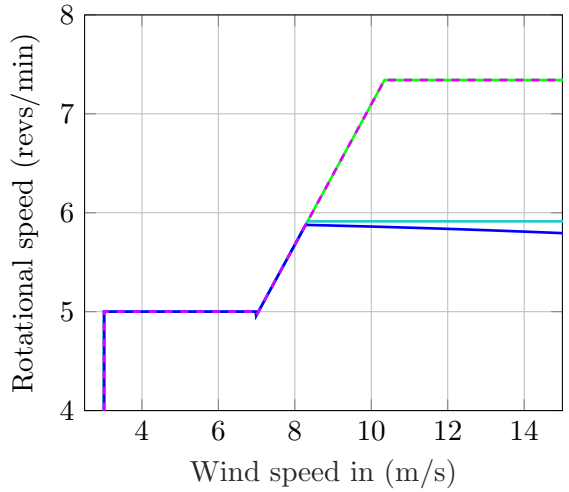

Figure 6: Rotational speed curve of IEA 15MW turbine. Clean: —, rough: - - -, ESM ROT 75 m/s: —, ESM REL 75 m/s: —

With the clean and rough airfoil polars, power curves for various erosion-specific operating conditions can be created. Figure 5 shows the mechanical power generated by the IEA 15MW turbine as a function of wind speed. In comparison to the clean power curve, rough turbine

operation sheds performance in the variable load region. Rated power production is, therefore, delayed to higher wind speeds. Additionally, two ESM power curves are given for the ROT and REL ESM at one particular ESM speed. When operating in the ESM the turbine loses substantially performance at rated power. Due to the maximum generator torque and reduced rotational speed, the maximum power of the turbine is significantly limited. There is also a power loss in the partial load region. It occurs when, as can be seen in Figure 6, the rotational speed is limited, but the torque can still continue to increase to the higher wind speeds. In the REL ESM the rated power of the turbine does not stay constant after the maximum generator torque has been reached. Due to the increasing wind inflow speed, the rotational speed has to decrease so that $U_{\mathrm{ESM,REL}} = \mathrm{norm}(U_{\mathrm{in}}, U_{\mathrm{rot}})$ stays constant. It should be noted that when the ESM is utilized, the resultant power curve of the turbine is a linear combination of the clean and the ESM power curve depending on the ESM frequency i.e. how often there is a *damaging rain event*. To conclude, LEE negatively affects the power production below rated capacity while operating in ESM sheds performance mainly at rated power of the turbine.

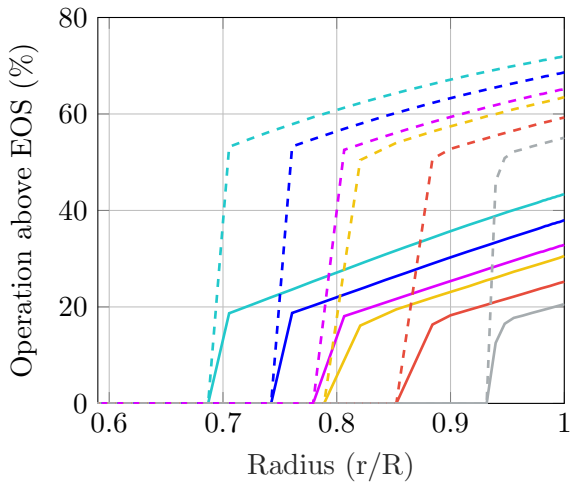

Figure 7: Percentage of operation above EOS. IEA 15MW: 5-65: ——, 5-70: ——, 5-75: ——, 10-65: - - -, 10-70: - - -, 10-75: - - - and NREL 5MW: 5-65: ——, 5-70: ——, 5-75: ——, 10-65: - - -, 10-70: - - -, 10-75: - - -. First number indicates mean wind speed, second number EOS, both in m/s.

Table 1: Strategy pairs of EOL in percentage span and ESM speeds for IEA 15MW and NREL 5MW turbine. Results for the ROT and REL droplet impact speed models are given.

Speed	ROT	REL	ROT	REL
	IEA 15 MW		NREL5MW	
65 ms^{-1}	69%	65%	79%	76%
70 ms^{-1}	74%	71%	85%	82%
75 ms^{-1}	78%	76%	93%	88%

This study uses a simplified erosion model that depends on a so-called Erosion Onset Speed (EOS). The assumption is made that a blade element will experience erosion when a rain droplet impacts at or above the EOS. The impact speed of the droplet is evaluated according to the 'ROT' and 'REL' rules explained before. The term damaging rain event is used to highlight that not all rain events might cause damage to the blade. Erosion is treated as binary property, meaning a blade element is either undamaged (clean) or eroded (rough). Different grades of erosion are not considered. By defining an EOS and a mean wind speed at a particular site, a graph can be created that shows for every blade element the probability of operation above the EOS (see Figure 7). It should be noted that the computed probabilities are independent of the turbines' polars and solely a function of the site conditions and the wind turbine control. Three EOS of 65, 70 and 75 m/s were chosen heuristically. In this study, it is assumed, for

simplicity, that erosion starts where the probability becomes nonzero. This position is coined Erosion Onset Location (EOL). The graph shows that a specific EOS will yield a unique EOL. The wind turbine operator can choose between two strategies, do nothing and accept erosion from the EOL outwards or limit the tip speed of the turbine to the EOS in the ESM to fully avoid erosion. Therefore strategy pairs of EOL and EOS can be found. They are tabulated in Table 1. It is important to compare these pairs when comparing erosion operating strategies to ensure fair results. While having interesting effects on the erosion onset and control of the turbine, an investigation into the REL mode showed that it did not have a meaningful impact on the conclusions of this paper with respect to the ROT mode. Therefore, the REL mode was omitted in the further discussion. At the EOL in Figure 7, the probability increases linearly and subsequently starts to flatten out. When comparing the results of the two turbines one can see that, for a fixed EOS, the IEA turbine starts to erode about 10 to 15 percent of span further inboard. For a mean wind speed of 10 m/s, the probability (around 50%) close to the EOL is similar for both turbines. In contrast, at the tip, the probability of the IEA turbine is about 10% higher. Based on these observations one can infer that the rate of erosion at the EOL should be similar for both turbines, but increases for the IEA turbine when moving along the blade towards the tip. Figure 7 shows that a decrease in mean wind speed does not change the EOL. An explanation is straightforward, when reducing the mean wind speed the probabilities of high wind speeds in the Weibull distribution reduce, but never become zero. Thus, in this simplified erosion model, the EOL is invariant with mean wind speed. Mean wind speed has, however, a significant effect on the height of the curves. At 5 m/s mean wind speed and 65 m/s EOS, the IEA turbine operates at its tip around 40% of the time above this threshold, with 10 m/s this probability increases to around 70%.

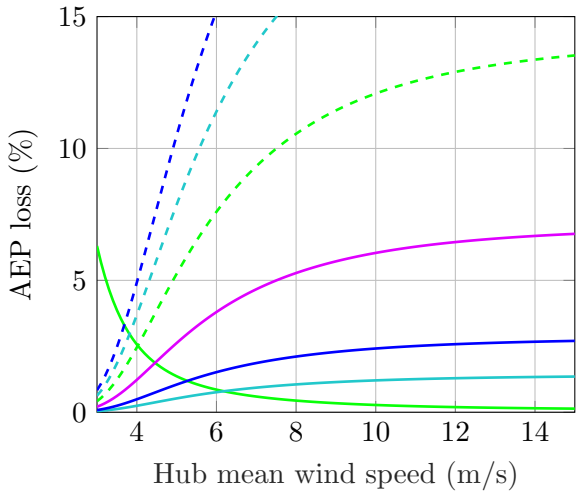

Figure 8: AEP loss due to LEE and ESM control for IEA 15MW turbine. LEE r/R 70%: —, ESM 65m/s frequency 5%: —, 10%: —, 25%: —, 50%: - - -, 75%: - - -, 100%: - - -

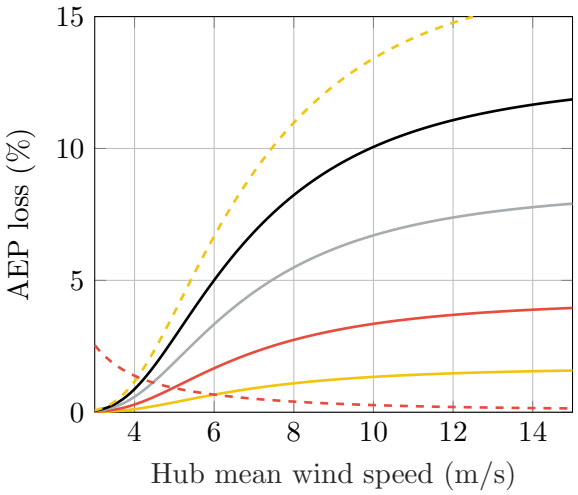

Figure 9: AEP loss due to LEE and ESM control for NREL 5MW turbine. LEE r/R 70%: - - -, ESM 65m/s frequency 10%: —, 25%: —, 50%: —, 75%: —, 100%: - - -

Figure 8 and 9 show the AEP loss as a function of the Weibull mean wind speed for the NREL and IEA turbine. The AEP loss was normalized with respect to the clean configuration. Two general types of lines can be seen: falling and rising lines. A falling line corresponds to an AEP loss due to erosion, whereas a rising line belongs to an AEP loss due to operation in the ESM.

Erosion is thus especially detrimental at low mean wind speeds, i.e. high probability of operation in the partial load region. On the contrary, operation in the ESM is very favourable at low wind speed, but leads to increased performance losses at high mean wind speeds. An intersection point between the erosion and ESM curve exists. At this point, both strategies lead to equal AEP loss. By plotting ESM curves of different ESM frequencies different intersection points are generated that either move up or down on the erosion curve. Recording the combination of the Weibull mean wind speed and the ESM frequency at which an intersection occurs leads to Figure 10.

A comparison between Figure 8 and 9 reveals that the IEA turbine has a higher loss due to LEE than the NREL turbine at low mean wind speed sites. This difference vanishes with higher wind speeds. At about 8 m/s mean wind speed the losses due to LEE are equal for both turbines. The effect of operating in the ESM is for the IEA turbine more severe also. These findings assume a constant erosion onset location of 70% and an ESM speed of 65 m/s. The IEA turbine shows more performance loss in the ESM due to its higher rated tip speed (95 m/s) than its NREL (80 m/s) counterpart. The higher susceptibility of the IEA turbine towards LEE can be explained by the aforementioned discussion of Figure 3 and 4. The NREL turbine has already at small angles of attack a transition point that is located at the very front of the leading edge. Thus, even in its clean configuration, it behaves already similar to an airfoil in rough condition. This is in contrast to the convex profile of the IEA turbine in Figure 4.

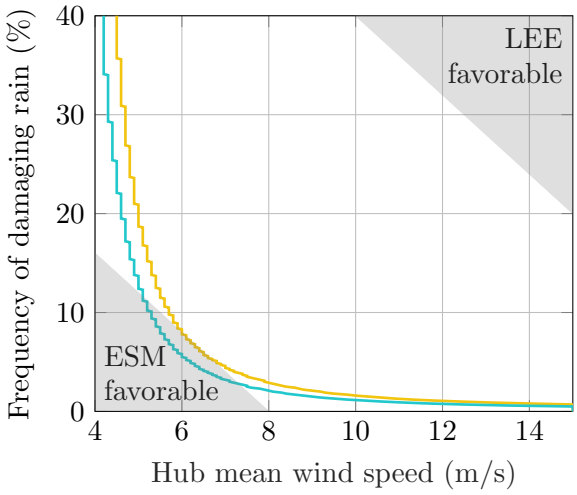

Figure 10: Intersection point of LEE and ESM for different rain frequencies and hub mean wind speeds. IEA 15MW: —, NREL 5MW: —

Figure 10 tracks the intersection point of ESM and LEE in the two-dimensional space spanned by the ESM frequency and the mean wind speed. When the operation point lies above the curve it is favorable to operate with LEE. In contrast, when the operation point lies below the curve it is more advantageous to utilize ESM. The curves of both turbines rapidly rise at low mean wind speeds. There is a practical limit at which operation in the ESM is always better than operation with LEE. It is defined by the intersection of the LEE curve and the 100% ESM curve as shown in Figure 8 and 9. The shape of the curve leads to a narrow band in its knee at which the most favourable mode of operation quickly changes. For example, the curve of the NREL turbine drops from about 7.5% frequency at 6 m/s speed to about 2.5% at 8 m/s. The allowable rain frequency for the ESM to be favorable is lower for the IEA turbine. This is interesting, since the IEA turbine shows a higher loss due to LEE. However, it is also more affected by the ESM, with the latter being dominant.

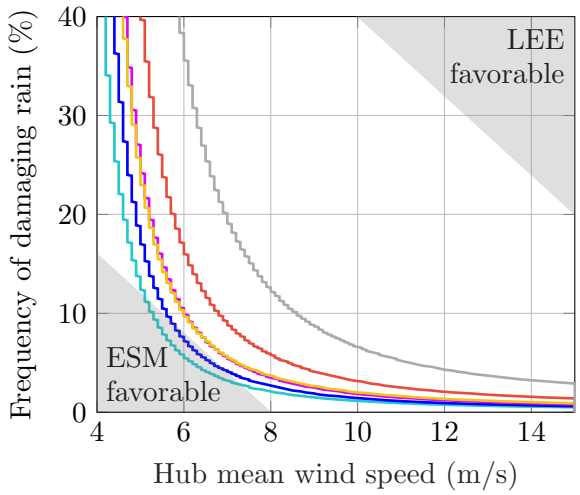

Figure 11: Intersection point of LEE and ESM for different ESM speeds at a fixed EOL of 70%. IEA 15MW: ROT65: —, ROT70: —, ROT75: — and NREL 5MW: ROT65: —, ROT70: —, ROT75: —

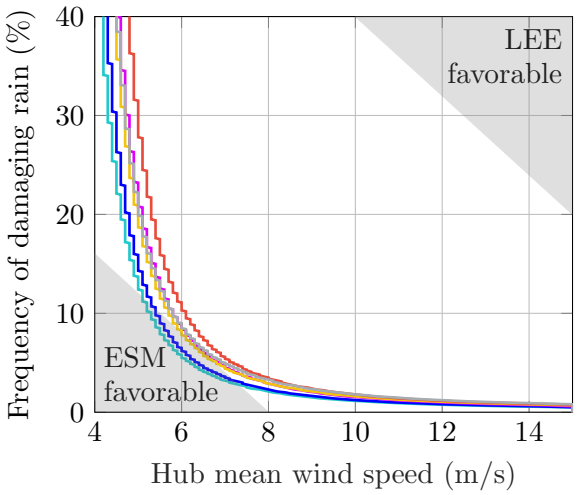

Figure 12: Intersection point of LEE and ESM for different ESM speeds. Simulation pairs according to Table 1 are used. IEA 15MW: ROT65: —, ROT70: —, ROT75: — and NREL 5MW: ROT65: —, ROT70: —, ROT75: —

Figure 11 shows the effect of different ESM speeds on the optimum mode of operation. In this plot, it is assumed that the erosion onset location sits at 70% span of the blade. As expected a higher ESM velocity shifts the entire graph up and to the right. When instead the pairs of Table 1 are considered, the curves move towards each other. This is shown in Figure 12. The curves only show a total shift of about 1 m/s of mean wind speed. Figure 13 gives an explanation for this. Two pairs of the NREL turbine are shown. With an increase in the EOS from 65 to 75 m/s both LEE and ESM loss curves move upward. However, their movement does not cause a shift in the intersection point itself. From the fact that the curves almost collapse onto each other, one can come to an interesting conclusion. Provided that the simplistic damage model of the EOS holds somewhat true, the optimum control strategy, i.e. whether to use LEE or ESM, is (almost) not influenced by the ESM speed, the erosion onset location and even the turbine type itself. The two parameters that matter (most) are the frequency of damaging rain and the mean wind speed of the site.

Figure 14 shows the effect of shear on the AEP loss due to blade erosion. The losses of the NREL turbine are essentially equal for all considered shear coefficients. For the IEA turbine, a shear coefficient of 0.4 does increase the erosion loss by about 0.5 to 1% for mean wind speeds below 7 m/s. For higher site speeds this difference is diminishing. Interestingly, at low wind speeds, shear coefficients of 0.1 and 0.2 actually decrease the AEP loss due to erosion.

In Figure 15 the influence of varying transition location on the AEP loss of the NREL turbine is shown. As shown in Figure 4, a lower value shifts the transition point of the clean baseline case upstream and, hence, reduces differences to the rough (eroded) case. This effect can be seen for mean wind speeds lower than 8 m/s. Overall, a faster natural transition is reducing the performance loss and, therefore, reduces the benefit of the ESM. The effect is of similar magnitude as for mean shear.

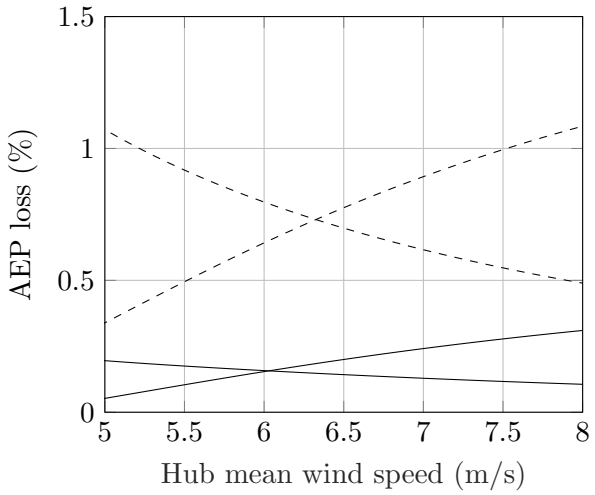

Figure 13: Shift in intersection point using simulation pairs of the NREL turbine with 10% ESM utilization. 65 m/s ROT pair: - - -, 75 m/s ROT pair: ——

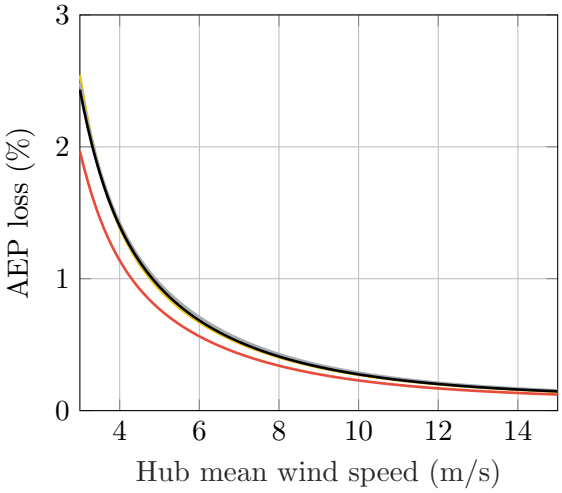

Figure 14: AEP loss due to LEE for different shear exponents. NREL: 0.0: ——, 0.1: ——, 0.2: ——, 0.4: ——

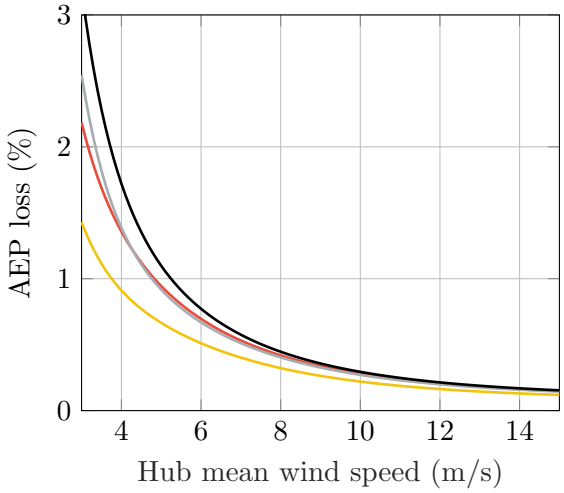

Figure 15: AEP loss due to LEE for different N-factors. NREL: N7: ——, N8: ——, N9: ——, N10: ——

4. Conclusions

In this study, the performance loss of operating with LEE and in the ESM was investigated for the IEA 15MW and NREL 5MW reference wind turbines. The performance loss was evaluated with simulations employing the free-vortex method CACTUS by comparing calculations with erosion against reference calculations with clean polars. Erosion was assumed to lead to rough polars. The polars were obtained using XFoil. For the computations, both site-specific and turbine-specific parameters were varied. The first set includes mean wind speed, damaging rain frequency and mean shear, whereas the second set includes erosion extent along the blades, critical speed for the onset of erosion and the transition location along the airfoil. The key takeaways of this study are:

- A break-even point for applying the ESM exists depending on the mean wind speed of the

site. The reason is that LEE negatively affects the power production below rated capacity, while operating in ESM predominantly sheds performance at rated power of the turbine.

- The break-even point strongly depends on the assumed frequency of damaging rain events. This is the most influential lever to make the ESM more attractive, e.g. by understanding better which rain events actually cause erosion and by better forecasting of these events. The effect of a possible correlation between rain frequency and site mean wind speed should be considered as well.
- The IEA 15MW reference turbine exhibits, in particular at lower wind speeds, a higher performance loss due to erosion than the NREL 5MW turbine. However, the break-even point for the ESM shows little sensitivity to the turbine design.
- From the impact of atmospheric conditions only mean shear was investigated and showed a similar impact as a change in the transition modeling. The impact on the above conclusions is considered small.

In conclusion, an erosion-optimal operation is strongly governed by the site characteristics and much less by turbine design, and the viability of an ESM strategy can be significantly expanded by a better understanding of blade damage mechanisms and improved forecasting of the related weather events.

References

[1] Herring R, Dyer K, Martin F and Ward C 2019 *Renewable and Sustainable Energy Reviews* **115** 109382 ISSN 1364-0321 URL `https://www.sciencedirect.com/science/article/pii/S1364032119305908`

[2] Bech J I, Hasager C B and Bak C 2018 *Wind Energy Science* **3** 729–748 URL `https://wes.copernicus.org/articles/3/729/2018/`

[3] Pathi K and Iungo G 2021 Quantification of power loss due to leading edge erosion through infrared-camera inspections and scada data analysis Wind Energy Science Conference

[4] Gaertner E, Rinker J, Sethuraman L, Zahle F, Anderson B, Barter G E, Abbas N J, Meng F, Bortolotti P, Skrzypinski W *et al.* 2020 Definition of the IEA 15-megawatt offshore reference wind turbine Tech. rep. National Renewable Energy Lab.(NREL), Golden, CO (United States)

[5] Jonkman J, Butterfield S, Musial W and Scott G 2009 Definition of a 5-MW reference wind turbine for offshore system development Tech. rep. National Renewable Energy Lab.(NREL), Golden, CO (United States)

[6] Drela M 2013 Xfoil 6.99 https://web.mit.edu/drela/Public/web/xfoil/

[7] Murray J and Barone M The development of cactus, a wind and marine turbine performance simulation code 49th AIAA Aerospace Sciences Meeting including the New Horizons Forum and Aerospace Exposition URL `https://arc.aiaa.org/doi/abs/10.2514/6.2011-147`

[8] Jonkman J and Buhl Jr M 2020 Wisdem - airfoilpreppy National Renewable Energy Lab.(NREL), Golden, CO (United States) https://github.com/WISDEM/AirfoilPreppy

[9] Viterna L A and Janetzke D C 1982 Theoretical and experimental power from large horizontal-axis wind turbines Tech. Rep. NASA-TM-82944 National Aeronautics and Space Administration, Cleveland, OH (USA). Lewis Research Center

[10] Chiu P, Barone M and Murray J C 2020 Cactus-tools Sandia National Laboratories Water Power Technologies https://github.com/SNL-WaterPower/CACTUS-tools